Laboratory Work No. 2. Alpha Decay. Interaction of Alpha Particles with Matter

The purpose of this laboratory work is to study the phenomenon of α decay, the mechanism of α particle formation, and interaction of α particles with matter.

Contents

1. α decay

α decay is the decay of atomic nuclei accompanied by the emission of α particles (isotope ^{4}He). Most α radioactive isotopes are located in the periodic table in the region of heavy nuclei ($Z > 83$). This is due to the fact that α

decay is associated with Coulomb repulsion, which increases with increasing nuclear size faster (as Z^2) than the attractive nuclear forces, which increase linearly with the mass number A.

A necessary requirement for α decay, as any other kind of decay, comes from the energy conservation law. The rest energy of the initial nucleus is equal to the sum of total energies of the products, which results in the following condition on the masses:

$$M(A,Z) > M(A-4,Z-2) + m_\alpha, \tag{1}$$

where $M(A,Z)$ and $M(A-4,Z-2)$ are the masses of the initial and final nuclei, respectively, m_α is the mass of the α particle. The decay energy released in the decay:

$$Q_\alpha = (M(A,Z) - M(A-4,Z-2) - m_\alpha)c^2, \tag{2}$$

is distributed between the decay products in the form of their kinetic energies.

In most cases, the main part of the α decay energy (about 98%) is carried away by the α particles. Using the conservation laws of energy and momentum for the kinetic energy of the α particle T_α, the following relation can be obtained.

$$T_\alpha = \frac{M(A-4,Z-2)}{m_\alpha + M(A-4,Z-2)} Q_\alpha \approx \frac{A-4}{A} Q_\alpha. \tag{3}$$

Nuclei can also undergo α decay to excited states of the final nuclei and from excited states of the initial nuclei. Therefore, relation (2) for the α decay energy can be generalized as follows:

$$Q_\alpha = (M(A,Z) - M(A-4,Z-2) - m_\alpha)c^2 + E_i^* - E_f^*, \tag{4}$$

where E_i^* and E_f^* are the excitation energies of the initial and final nuclei, respectively.

An important property of α decay is that a small change in the energy of

α particles greatly affects the half-lives, often by many orders of magnitude. For example, for isotope ^{232}Th, $Q_\alpha = 4.08$ MeV, $T_{1/2} = 1.41 \cdot 10^{10}$ years, while for ^{218}Th $Q_\alpha = 9.85$ MeV, $T_{1/2} = 10$ μs. A change in energy by a factor of 2 corresponds to a change in half-life by 24 orders of magnitude.

For most nuclei with $A > 190$ and for many nuclei with $150 < A < 190$, condition (1) is satisfied. However, not all of them are considered α radioactive. For example, all natural isotopes of europium (^{151}Eu, ^{153}Eu), tungsten (^{180}W, ^{182}W, ^{183}W, ^{186}W), bismuth (^{209}Bi), lead (^{204}Pb, ^{206}Pb, ^{207}Pb, ^{208}Pb) have positive α decay energies. But due to the small values of Q_α and, accordingly, small decay probabilities, it is not always possible to detect it, and even less so to determine the half-lives. Nevertheless, the development of experimental methods has made it possible to measure the half-lives of up to $\sim 10^{19}$ years, such as of ^{180}W: $Q_\alpha = 2.508$ MeV, $T_{1/2} = 1.8 \cdot 10^{18}$ years and of ^{206}Bi: $Q_\alpha = 3.531$ MeV, $T_{1/2} = 1.9 \cdot 10^{19}$ years.

For even-even isotopes of the same element (that is, isotopes with an even amount of protons and even amount of neutrons), the dependence of the half-life on the α decay energy is well described by the empirical Geiger-Nuttall law that reads:

$$\lg T_{1/2} = A + B/(Q_\alpha)^{1/2}, \tag{5}$$

where A and B are coefficients weakly depending on Z. Taking into account the charge of the daughter nucleus Z, the relationship between the half-life $T_{1/2}$ and the α decay energy Q_α can be represented in the form

$$\lg T_{1/2} = 9.54 \frac{Z^{0.6}}{\sqrt{Q_\alpha}} - 51.37, \tag{6}$$

where $T_{1/2}$ is in seconds, Q_α is in MeV.

Fig. 1 shows experimental half-life values for 119 α radioactive even-even nuclei (Z from 74 to 106) and their description using relation (6).

For odd-even, even-odd, and odd-odd nuclei, the general trend remains, but their half-lives are 2 to 1000 times greater than for even-even nuclei with the same Z and Q_α.

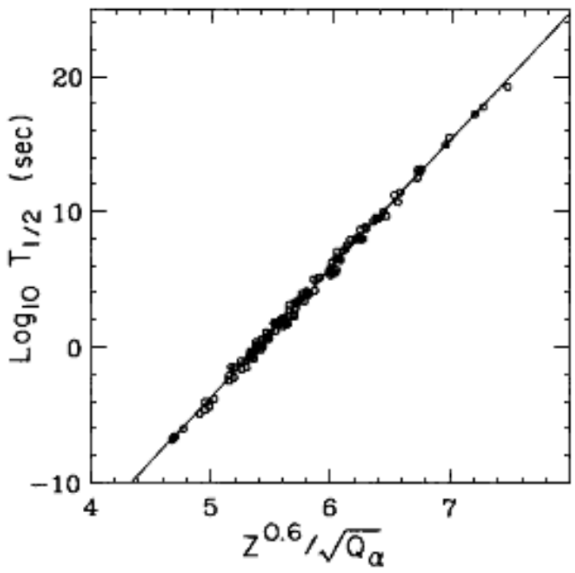

Figure 1. Experimental half-lives and their description using relation (6)

The main features of α decay, in particular the strong dependence of the probability on energy, were explained by G. Gamow in 1928. He showed that the probability of α decay is mainly determined by the probability of the α particle passing through the potential barrier. Let us consider Gamow's model of α decay. It is assumed that the α particle moves in a spherical region of radius R, where R is the radius of the nucleus. That is, in this model, it is assumed that the α particle constantly exists in the nucleus.

The probability of α decay λ is equal to the product of the probability of finding the α particle at the nuclear boundary f and the probability of its passage through the potential barrier D (barrier transparency).

$$\lambda = fD = \frac{\ln 2}{T_{1/2}}. \tag{7}$$

The value f can be identified with the number of collisions per unit time that the α particle experiences with the inner boundaries of the barrier, which can be estimated as

$$f = \frac{v}{2R} \approx \frac{v}{2r_0 A^{1/3}} \approx \frac{c}{2r_0 A^{1/3}} \left(\frac{2(T_\alpha + V_0)}{\mu_\alpha c^2} \right)^{1/2}. \tag{8}$$

Here, v is the speed of the α particle inside the nucleus, V_0 is the depth of

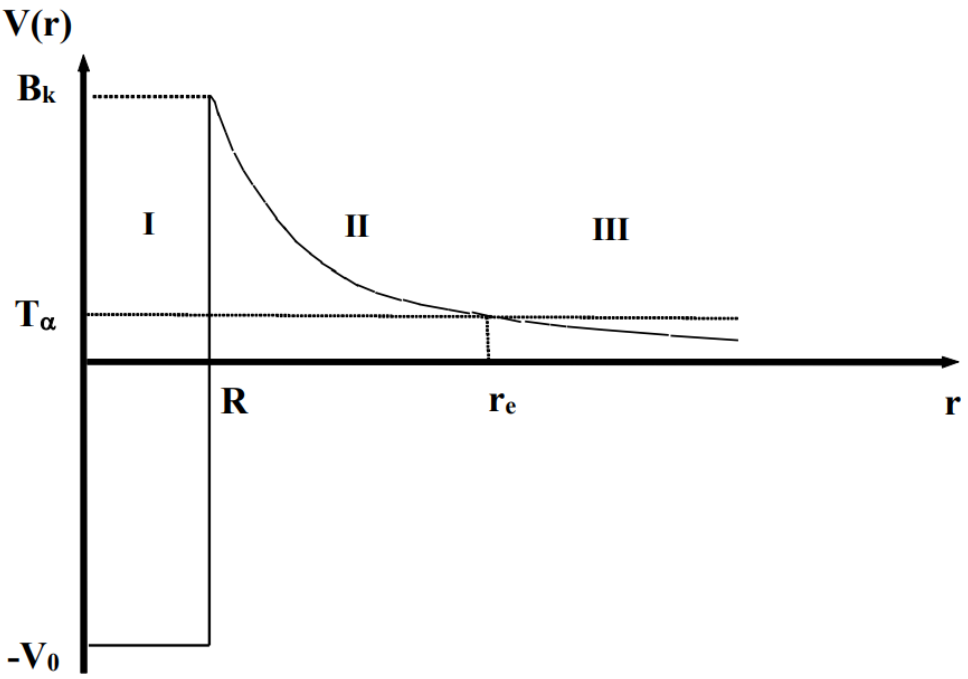

Figure 2. Dependence of the potential energy of interaction between the α particle and the residual nucleus on the distance between their centers

the nuclear potential, μ_α is the reduced mass of the α particle given by the formula

$$\mu_\alpha = \frac{m_\alpha M(A-4, Z-2)}{m_\alpha + M(A-4, Z-2)}, \tag{9}$$

and T_α is the kinetic energy of the α particle determined by relation (3). Substituting $V_0 = 35$ MeV, $T_\alpha = 5$ MeV into expression (8), we obtain for nuclei with $A \approx 200$, $f \approx 10^{21}$ s^{-1}.

Fig. 2 shows the dependence of the potential energy between the α particle and the residual nucleus on the distance between their centers. The Coulomb potential is cut off at a distance R, which is approximately equal to the radius of the residual nucleus – for small distances from the center, the nuclear strong forces greatly contribute to the overall potential. The height of the Coulomb barrier B_k is determined by the relation.

$$B_k = \frac{zZe^2}{R} \approx \frac{zZe^2}{r_0 A^{1/3}} \approx \frac{2Z}{A^{1/3}} \text{ MeV}. \tag{10}$$

Here Z and z are the charges (in units of the elementary charge e) of the

residual nucleus and the α particle, respectively, $r_0 \approx 1.3$ fm. For example, for ^{238}U $B_k \approx 30$ MeV.

Three regions can be distinguished:

1) $r < R$ – a spherical potential well of depth V_0. In classical mechanics, an α particle with kinetic energy $T_\alpha + V_0$ can move in this region but cannot leave it. In this region, the strong interaction between the α particle and the residual nucleus is essential;

2) $R < r < r_c$ – the region of the potential barrier, where the potential energy is greater than the energy of the α particle, i.e., this is a region forbidden for a classical particle;

3) $r > r_c$ – the region outside the potential barrier.

In quantum mechanics, the passage of an α particle through the barrier (an effect known as quantum tunneling) is possible. The probability D of a particle passing through the barrier (the barrier transparency coefficient) is determined by the relation:

$$D = \exp\left[-2\int_R^{r_c}\sqrt{\frac{2\mu}{\hbar^2}(V(r)-Q_\alpha)}dr\right]. \qquad (11)$$

The half-lives calculated by formulas (7), (8) and (11) correctly convey the most important pattern of α decay: the strong dependence of the half-life $T_{1/2}$ on the energy of the α particles T_α (or the α decay energy Q_α). When the half-lives change by more than 20 orders of magnitude, the differences between the experimental values and the calculated ones are only 1–2 orders of magnitude.

Of course, such discrepancies are still quite large. What is their source and how should the theory be improved to reduce these discrepancies with experiment? What factors should be additionally taken into account?

The formulas given above describe the emission of α particles with zero orbital angular momentum l_α. However, decay with non-zero orbital angular momentum is also possible; moreover, in some cases, decay with $l_\alpha = 0$ is

forbidden by conservation laws. In this case, the centrifugal potential $V_l(r)$ is added to the Coulomb potential $V_k(r)$.

$$V(r) = V_k(r) + V_l(r), \tag{12}$$

$$V_l(r) = \frac{\hbar^2 l(l+1)}{2\mu_\alpha r^2}. \tag{13}$$

Although the height of the centrifugal barrier for heavy nuclei at $l = 8$ is only about 10% of the height of the Coulomb barrier and the centrifugal potential decreases faster than the Coulomb one, the effect is quite noticeable and for large l can lead to suppression of α decay by more than 2 orders of magnitude.

Furthermore, the results of barrier transparency calculations are sensitive to the mean radii of the nuclei R. For example, a change in R of only 4% leads to a change in the half-life $T_{1/2}$ by a factor of 5. Nuclei with $A \geq 230$ can be strongly deformed, which leads to α particles preferring to fly out along the major axis of the ellipsoid, and the average probability of emission differs from that for a spherical nucleus. The strong dependence of the half-life on the nuclear radius can be used to determine the radii of nuclei from experimental half-life values.

Finally, the considered model did not take into account the structure of the states of the initial and final nuclei and the closely related problem of the formation of the α particle in the nucleus, the probability of which was silently assumed to be 1. More sophisticated models take these finer details into account.

In Table 1, we show some data related to select α radioactive isotopes.

Table 1. Characteristics of some α radioactive nuclei

Nucleus	Energy of α particles, MeV	Fraction of this decay branch	Half-life
^{238}U	4.15	23%	$4.468 \cdot 10^9$ y
	4.2	77%	
^{226}Ra	4.6	5.4%	1600 y
	4.78	94.6%	
^{233}U	4.78	14.6%	$1.592 \cdot 10^5$ y
	4.82	83%	
^{239}Pu	5.1	73%	24119 y
	5.14	15.1%	
	5.16	11.5%	
^{210}Po	5.3	$\sim 100\%$	138.376 d
^{238}Pu	5.46	28%	87.74 y
	5.5	72%	
^{244}Cm	5.76	23%	18.11 y
	5.80	77%	
^{252}Cf	6.08	15.7%	2.645 y
	6.12	84.2%	
^{288}Mc	10.3	100%	0.17 s

For isotopes with several decay branches, different branches are related to decays on different states of the daughter nucleus. Examples of such decays are shown for isotopes ^{238}U and ^{239}Pu in Fig. 3.

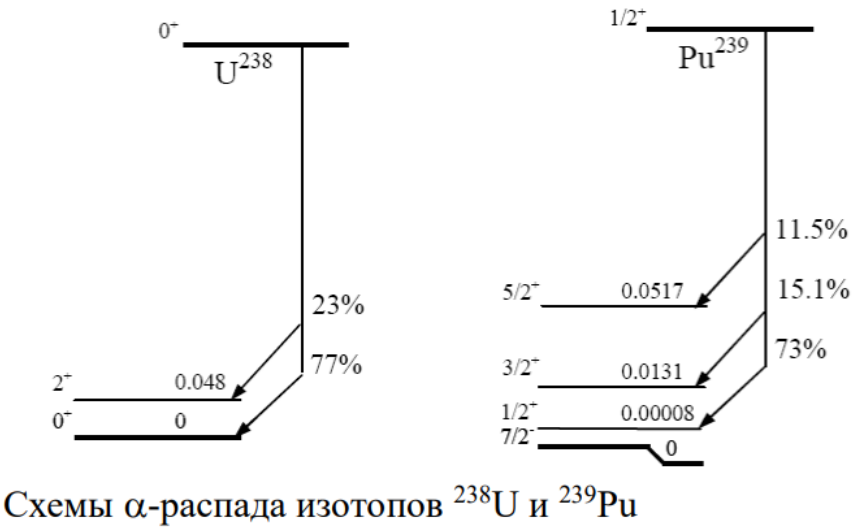

Figure 3. Diagrams of α decay of isotopes ^{238}U and ^{239}Pu

2. Radioactive families

Under natural conditions on Earth, there are about 40 α radioactive isotopes, which are combined into three radioactive series, starting with ^{236}U ($A = 4n$), ^{238}U ($A = 4n + 2$), ^{235}U ($A = 4n + 3$). With some stretch (since the isotopes of this series have had time to decay during the existence of the Earth), a fourth series can be added, which begins with ^{237}Np ($A = 4n + 1$). After a series of successive decays, stable nuclei with a number of protons and neutrons close or equal to the magic numbers ($Z = 82, N = 126$) are formed, namely ^{208}Pb, ^{206}Pb, ^{207}Pb, ^{209}Bi. α decays are interspersed with β decays, since after α decays the final nuclei are increasingly farther from the line of β stability, i.e., they are neutron-rich.

A simplified decay chain of the radioactive series ($A = 4n+2$) is presented on Fig. 4. All of the α decays are shown with arrows pointing straight down, while β decays are shown with arrows pointing diagonally to the right. Half-lives, α decay energies Q_α and branching ratios are also shown.

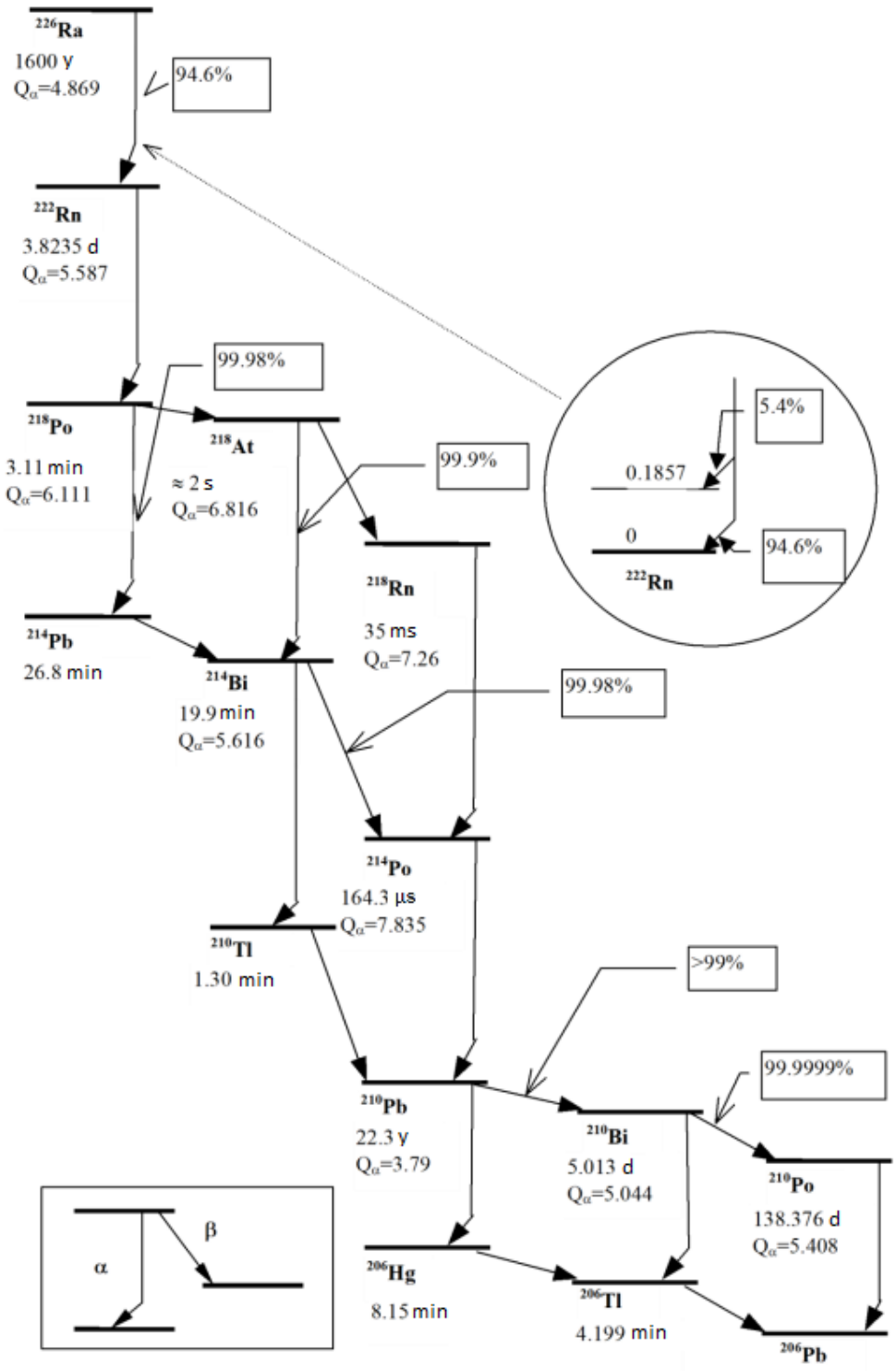

Figure 4. Simplified decay chain of the radioactive series ($A = 4n + 2$), starting from ^{226}Ra. The energies of α decay Q_α are given in MeV. The figure also shows the half-lives of the resulting radioactive isotopes and the probabilities of the main decay channels

3. Interaction of α particles with matter

When passing through matter, a heavy charged particle loses kinetic energy due to ionization and excitation of the atoms of the substance. These losses determine the particle's range. The probability of ionization of medium atoms at energies of several MeV is approximately 10^3 times greater than the probability of nuclear interaction. The magnitude of ionization losses, due to the Coulomb interaction of the passing particle of charge ze with the electrons of the substance, is determined mainly by said charge, velocity v, and the electron density in the substance n_e. The magnitude of ionisation energy loss per unit path length is described by the Bethe-like expression (in a simplified form):

$$-\left(\frac{dT}{dx}\right)_{\text{ion}} = \frac{4\pi e^4 z_1^2}{m_e v^2} ZNB, \tag{14}$$

where $z_1 e$ is the particle charge, v its velocity, N the number density of atoms in the absorber (atoms per cm^3), Z the atomic number of the absorber, m_e the electron mass, and B is a slowly varying logarithmic function (the stopping number) which depends on velocity, the mean ionisation potential of the absorber atoms, and the reduced mass of the interacting particles. In the non-relativistic energy range the influence of the logarithmic factor B on the energy dependence of ionisation losses is weak, so that roughly

$$-\left(\frac{dT}{dx}\right)_{\text{ion}} \sim \frac{1}{v^2}.$$

The specific energy loss is proportional to the number of electrons in the substance and the square of the charge of the particle losing energy to ionization. The specific energy loss does not depend on the mass M of the particle passing through the substance (provided $M >> m_e$), but significantly depends on the particle's velocity. Therefore, with decreasing velocity, the specific losses of a charged particle in the substance increase.

In one ionization act in air, an α particle loses about 35 eV. That is, if the initial kinetic energy of the α particle is 4 MeV, it will completely stop

as a result of $4 \cdot 10^6/35 \cong 10^5$ ionization acts.

The interaction of α particles with the nuclei of the substance mainly reduces to Coulomb scattering at small angles. Thus, when moving in a medium, charged particles with the indicated energy will gradually slow down over a range length R, the trajectory of such a particle in the medium is generally rectilinear, and the range is determined by the integral.

$$R = \int_0^{T_0} \frac{\mathrm{d}T}{\mathrm{d}T/\mathrm{d}x}. \tag{15}$$

The range R is measured in centimeters or in units of mass thickness ρ (g/cm^2).

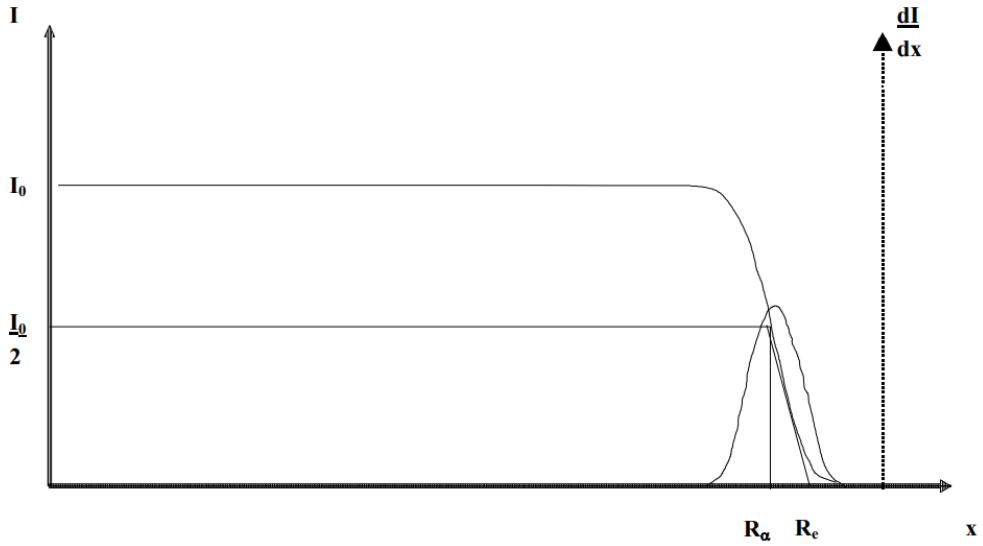

Figure 5. Dependence of the intensity of the alpha-particle flux in the medium on the distance between the source and the detector

The mean range R_α is defined as the thickness of the substance layer upon passing through which half of the particles are absorbed (see Fig. 5). The concept of the extrapolated range R_e is also sometimes used. It is determined by extrapolation along the tangent to the range curve from the point corresponding to the absorption of half of the particles. As can be seen from Fig. 5, the ranges have a spread around the mean (known as the range straggling), described by a Gaussian function. Range straggling comes as a result statistical fluctuations in ionization losses. Indeed, if the average number of

ions produced by an α particle over its range length is N, then the root mean square deviation from this number will be $\sqrt{N}$, as per the Poisson distribution. Furthermore, when passing through the substance, the α particle can undergo charge exchange, turning into a singly charged helium ion ($^4He^+$) or a helium atom (^4He). The different charge of the particle along the entire path causes additional fluctuations in ionization and, consequently, in the range.

The mean range in air at room temperature and normal pressure for α particles with energy of 2-10 MeV is related to the energy by the empirical formula

$$R_\alpha(\text{cm}) = 0.32 \cdot T_\alpha^{3/2}(\text{MeV}). \tag{16}$$

4. Experimental setup

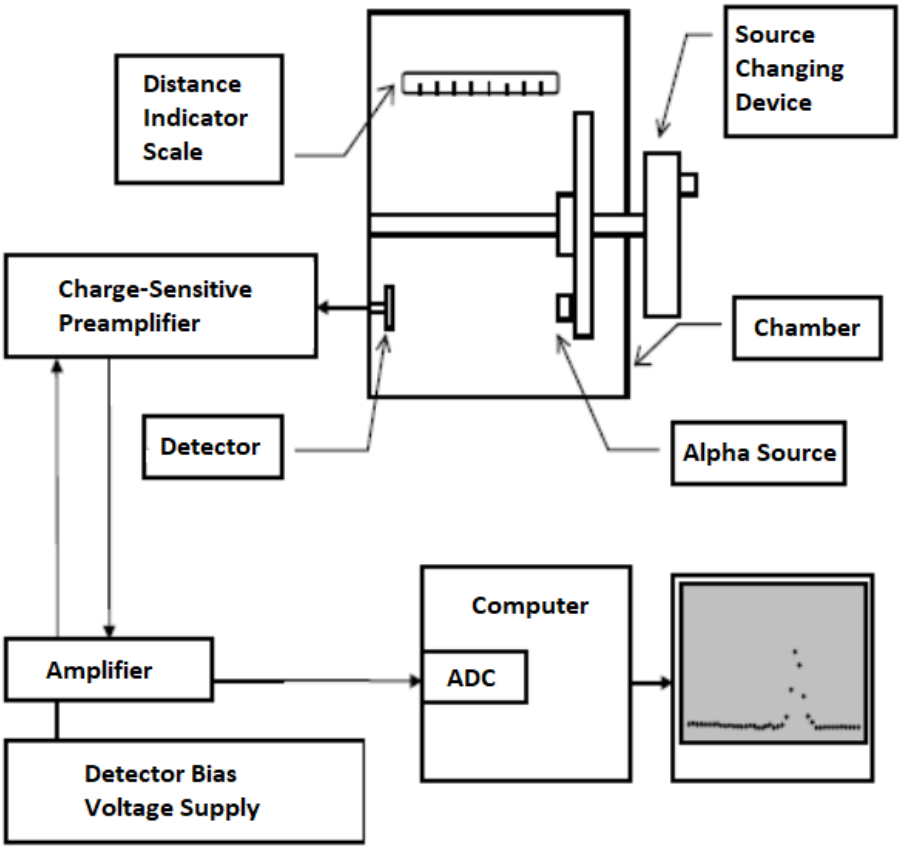

Figure 6. Block diagram of the setup

The block diagram of the experimental setup used in the current lab work

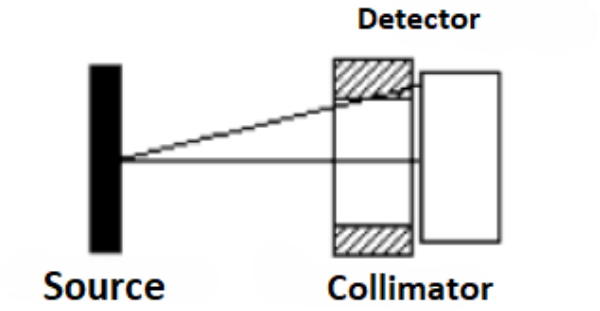

Figure 7. Geometry of the source, collimator, and detector

is shown in Fig. 6. The setup consists of a chamber with three α sources, a silicon detector, and recording electronic equipment. A semiconductor silicon detector is used as registering equipment in the setup. The sources are placed on a turret which has three fixed rotation positions and can be moved in the chamber relative to the detector. α particles emitted by the α radioactive isotopes, go through a narrow opening called a collimator, so that a narrow beam of particles travelling in a small solid angle, is registered by the detector (see Fig. 7). This is done so that α particles travelling at different angles pass through almost the same amount of absorbing material (air in this case) before reaching the detector. In the measurement mode, the chamber lid must be closed to prevent light from falling on the detector.

The electronic recording equipment consists of a charge-sensitive preamplifier and an amplifier. The charge-sensitive preamplifier is used to convert information about the charge generated in the sensitive region of the detector into the pulse amplitude. The amplifier amplifies and shapes the signals to improve the signal-to-noise ratio. Pulses from the amplifier go to an analog-to-digital converter (ADC). The ADC is used to measure the pulse amplitudes, i.e., to convert analog information into digital. It generates a number linearly dependent on the amplitude of the input signal.

An event processed by the ADC is recorded in the corresponding memory cell (channel) corresponding to a certain amplitude range. The channels are sequentially numbered so that larger amplitudes correspond to larger channel numbers. As statistics are accumulated, a distribution of channel number vs. number of events (the α decay spectrum) is formed in the computer memory,

which can be observed on the monitor or printed after the measurements.

4.1. Semiconductor detectors

Semiconductor detectors are widely used for detection and spectrometry-related measurements of charged particles and γ-quanta due to their high energy resolution, short signal rise time, and small size. Semiconductor detectors are usually made of silicon or germanium. In a semiconductor detector (Fig. 8), a depleted (sensitive) region is created, in which there are no free charge carriers. Upon entering the depleted region, an ionizing particle creates a significant number of charge carrier pairs, forming a thin cylinder of electron and hole plasma along the track.

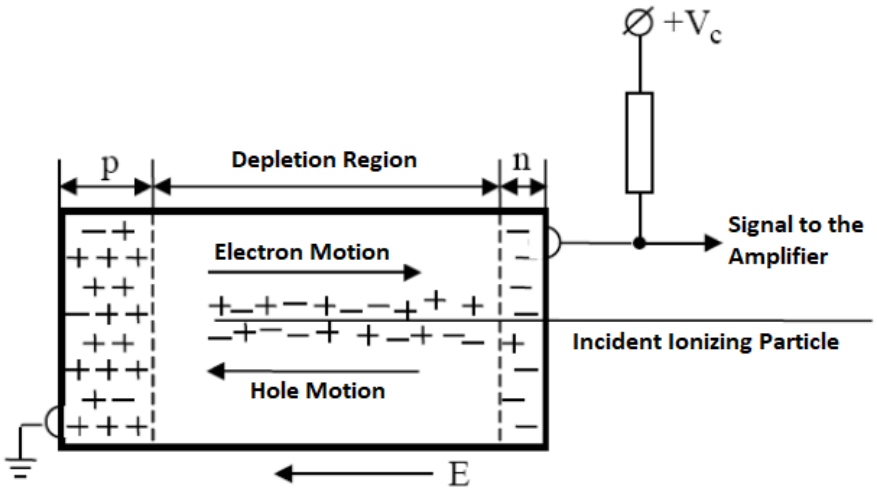

Figure 8. Circuit diagram of a semiconductor detector

The thickness of the depleted region in silicon detectors ranges from 10 μm to about 5 mm. It can be said that a semiconductor detector is a solid-state (crystalline) ionization chamber.

On average, 3.6 eV is spent to create one electron-hole pair in silicon, regardless of the energy, mass, and specific losses of the primary particle. For comparison, the energy required to create one ion pair in gas ionization chambers is about 35 eV, and in a scintillation detector, about 350 eV is needed to generate one photoelectron. Since the statistical accuracy of en-

ergy measurement is determined by the number of generated charge carriers N (standard deviation equals $\sqrt{N}$), the energy resolution of semiconductor detectors is significantly higher than that of others. The input window of the detector is usually made very thin (20 – 100 $\mu g/cm^2$), and the incident particles therefore lose a negligible fraction of their energy in it.

The free charge carriers generated by the ionizing particle in the depleted region will move in the applied electric field, collecting on the electrodes (Fig. 8). The number of electron-hole pairs is proportional to the energy loss of the particle. To measure the energy of a particle, it is necessary that it loses all its energy and stops in the sensitive region. Note that when an electron and related hole move simultaneously, the total charge transferred is equal to one elementary charge, and not two.

The collected charges form a current pulse, the integral of which carries information about the energy that the particle lost in the sensitive region. The current pulse from the detector goes to the charge-sensitive preamplifier. In the charge-sensitive preamplifier, the current pulse is converted into a voltage pulse, the amplitude of which is proportional to the particle energy.

5. Experimental procedure

The two goals of the current lab work include identification of several unknown α radioactive isotopes and confirmation of the empirical relation (16) describing the range of α particles propagating in the air.

Exercise №1. Calibration of the spectrometer and identification of isotopes by α particle energies

As mentioned earlier, the ADC assigns each event a channel corresponding to a certain amplitude range. The channels are sequentially numbered so that larger amplitudes correspond to larger channel numbers n. As larger amplitudes are generated by α particles with higher energy, larger channel numbers correspond to events of registration of said α particles with higher

energy T_α. The dependence for our setup is linear:

$$T_\alpha = kn + b, \tag{17}$$

where k and b are some parameters. These parameters can be determined through the calibration procedure. Specifically, one can measure an isotope (^{226}Ra in this case) with a known spectrum, aka, known energies of α particles, and check which energies correspond to which channel numbers. Approximation with the linear dependence then yields the coefficients k and b. After the calibration procedure is over, unknown α radioactive isotopes can be determined by measuring the energies of α particles emitted in the process of their decay.

And so, the steps for this exercise are:

1) Install the ^{226}Ra source and bring it as close as possible to the detector.

2) Measure the energy spectrum of alpha particles from the ^{226}Ra source.

3) On the obtained spectrum, identify five peaks corresponding to alpha particles with known energies: 4.782, 5.305, 5.490, 6.002 and 7.687 MeV. Note that the presence of 5 peaks has to do with ^{226}Ra undergoing a chain of radioactive decays, resulting in creation of multiple α radioactive isotopes.

4) For each peak, determine its position in the spectrometer channels.

5) Plot a graph of the energy T_α (MeV) versus the channel number n (the calibration curve).

6) Approximate the obtained dependence with a linear function.

7) Install the unknown sources one by one and measure their α spectra without changing the source position.

8) Using the calibration curve, determine the energies of the α particles for each peak in the spectra of the unknown sources.

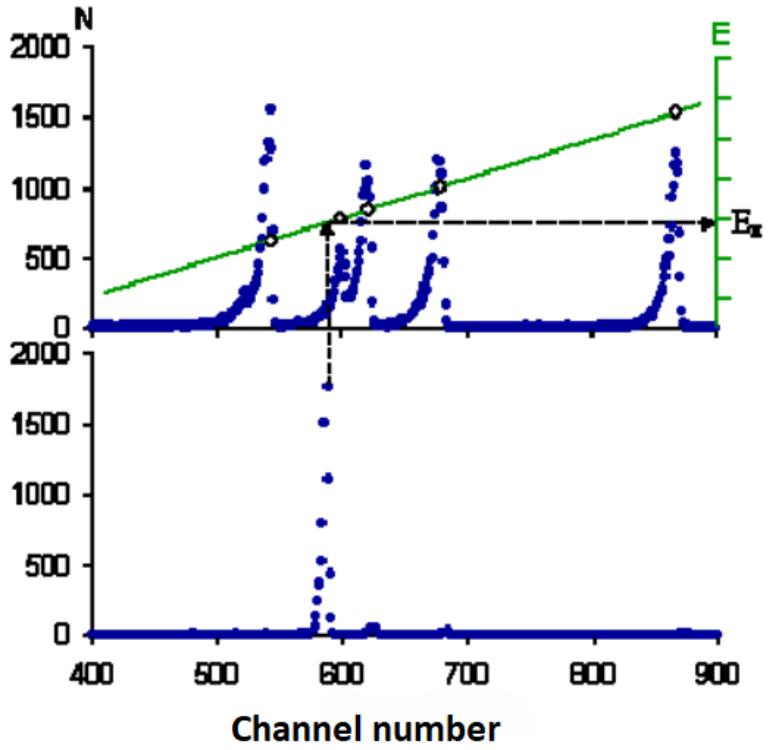

Figure 9. The upper part of the figure shows the spectrum of alpha particles from ^{226}Ra and its decay products, the lower part shows the alpha spectrum of an unknown source

9) Using the found energies and Table 1, identify the isotopes in the unknown sources.

10) Present the measurement and analysis of the results in the form of graphs similar to Fig. 9.

An example of obtained graphs is shown on Fig. 9.

Exercise 2. Investigation of the range of α particles in air

To study the dependence of the range of α particles on their kinetic energy, we will require to change the thickness of the absorbing material. As this task will have just air as the absorber, the experimental setup is made in such a way that the source of α particles can be moved relative to the detector. The previously used sample of ^{226}Ra is perfect for our purposes as it emits α particles of various energies, which should naturally have different ranges in the air.

Procedure:

1) Install the ^{226}Ra source.

2) Bring the source as close to the detector as possible (mark "0" on the scale).

3) Sequentially increase the distance between the source and the detector.

4) At each step, measure the spectrum. Measurement step:

   - On the initial section (before a noticeable drop in intensity) — every 2 mm.
   - On the section of sharp intensity drop — every 1 mm.

5) Continue measurements until the signal practically disappears.

6) For each of the five alpha lines of ^{226}Ra, plot the intensity (count rate) versus distance.

7) From each graph, determine the range R_α in air for particles of the corresponding energy, as the distance at which the intensity drops by half.

8) Plot the range R_α (cm) versus energy E_α (MeV).

9) Using the formula $R_\alpha = kT_\alpha^{3/2}$, determine the coefficient k from your experimental data.

10) Estimate the accuracy of determining k.

11) Compare the obtained value of k with the data from the empirical formula (16).

Important note: One should bear in mind that "0" corresponds to a certain distance between the source and the detector, which may not be absolute zero.

To submit the work, provide:

1) the graphs of measured spectra;

2) the calibration curve;

3) the energies of α lines and their assignment to specific isotopes that emit them;

4) the graph of the dependence of intensity of the α particle peaks on the thickness of the air layer between the α source and the detector;

5) an estimate of the coefficient k in the empirical dependence $R_\alpha(T_\alpha)$.